Deep Physical Informed Neural Networks for Metamaterial Design

ZHIWEI FANG [1] **AND JUSTIN ZHAN** [2]

[1]Department of Mathematical Sciences, University of Nevada, Las Vegas, NV 89154-4020, USA
[2]Department of Computer Science and Computer Engineering, University of Arkansas, Fayetteville, AR 72701, USA

Corresponding author: Justin Zhan (jzhan@uark.edu)

ABSTRACT In this paper, we propose a physical informed neural network approach for designing the electromagnetic metamaterial. The approach can be used to deal with various practical problems such as cloaking, rotators, concentrators, etc. The advantage of this approach is the flexibility that we can deal with not only the continuous parameters but also the piecewise constants. As our best knowledge, there is no other faster and much efficient method to deal with these problems. As a byproduct, we propose a method to solve high frequency Helmholtz equation, which is widely used in physics and engineering. Some benchmark problems have been solved in numerical tests to verify our method.

INDEX TERMS PINN, activation function, metamaterial design, electromagnetic cloaking, Maxwell's equation.

I. INTRODUCTION

Metamaterial is a kind of artificial electromagnetic materials which can control electromagnetic field in an unconventional manner. In the last decade, the electromagnetic metamaterials have experienced a significant development and attracted much attention among physicists, engineers, and mathematicians [1]–[3]. Their extraordinary properties, such as negative refraction, ultra refraction, and anomalous dispersion, cannot be found in nature and have been widely used in medicine, high-energy physics, and manufacturing industry, etc. [**?**], [4] proposed a spatial transformation method to distort the light trajectories around a barrier, then the cloaking has been achieved. The form invariance of Maxwell's equations play a big role in this work. This technique has then been used to design other metamatierials' properties such as rotators and concentrators. However, there are many open questions. For example, whether we can achieve perfect cloaking still remains unsolved.

Traditional numerical methods, such as finite element methods, only take care how to solve the PDE efficiently, and cannot discover the design of the metamaterial for a specific propose. Optimal control method may solve this problem, but it will take a lot of time and may not converges. Even for continuous parameters design problems, the optimal control

method requires complicate 1st order conditions (PDEs) and very fine mesh, and no guarantee for convergence. Let alone the piecewise constant problems, which makes a lot of senses in engineering and manufacturing industry. We therefore resort to a flexible numerical method to resolve the metamaterial design problem in practical applications.

The dramatic growth of available data and the evolution of deep learning [5] revolutionize our understanding of the physical world in modern application areas such as image recognition [6], drug discovery [7], and bioinformatics [8]. [9] studied physics informed neural networks (PINNs), which is a powerful tool for solving partial differential equations (PDEs) and their inverse problems. After that, several works have been published to discover more applications. Although we have many numerical methods to solve a PDE, it is usually hard to solve inverse problems of PDEs due to their low regularities and nonlinearities. So this enlighten us to try PINNs methods for inverse problems of PDEs, and lead us to the main topic of this paper: the metamaterial design problems via PINNs approach.

In this paper, we consider a general framework of the metamaterial design problems, including cloaking, rotators, and concentrators etc. All of them can be widely used in scientific areas. For example, the fighter airplanes with designed cloak coating may escape the radar detection. Designing rotators can help us deal with electromagnetic signal much more flexible and develop application-driven photonic devices. In the

following sections, we mainly focus on the cloaking and rotators problems. As our best knowledge, our method now is the most efficient one to solve these problems with high flexibility.

In particular, this paper devotes to solve frequency domain Maxwell's equation and the metamaterial design problems by using deep physical informed neural network (DPINN). The paper is organized as follows: In the second section, we introduce the DPINN method for solving frequency domain Maxwell's equation with high wave number. We have adopted the idea introduced in [2], [9] but we come up with a modified activation function to conquer the non-convergence phenomenon. In the third section, we introduce our model for the metamaterial design problems. In the forth section, we show a discrete design for cloaking problem and our experimental results. We make a conclusion in the last section.

II. RELATED WORK

A. PHYSICAL INFORMED NEURAL NETWORK FOR FREQUENCY DOMAIN MAXWELL'S EQUATION

As shown in [9], the PINNs can solved a wide class of PDEs, including Burger's equation, Shrödinger's equation and Navier-Stokes' equation and so on. This gives us more flexibility to study the theoretical and numerical behavior of PDEs. In this paper, we care about the frequency domain Maxwell's equation.

B. FREQUENCY DOMAIN MAXWELL'S EQUATION

Let $\Omega \subset \mathbb{R}^2$ be a bounded open set. Consider the following frequency domain Maxwell's equation on Ω:

$$\Delta E + k^2 E = 0 \quad \text{in } \Omega$$
$$E = E_w \quad \text{on } \partial\Omega \qquad (1)$$

where $E(x, y)$ is the electronic field in frequency domain depend on spatial variables x and y, k is the wave number and $E_w(x, y)$ is the given source wave. Δ is the Laplace operator, which defined by:

$$\Delta E(x, y) = \frac{\partial^2}{\partial x^2} E(x, y) + \frac{\partial^2}{\partial y^2} E(x, y)$$

We also define the curl operator $\nabla \times$ which will use below. For a vector function $\boldsymbol{E} = (E_x, E_y, E_z)$ in $\mathbb{R}^3$,

$$\nabla \times \boldsymbol{E} = \left(\frac{\partial E_z}{\partial y} - \frac{\partial E_y}{\partial z}, \frac{\partial E_x}{\partial z} - \frac{\partial E_z}{\partial x}, \frac{\partial E_y}{\partial x} - \frac{\partial E_x}{\partial y} \right)$$
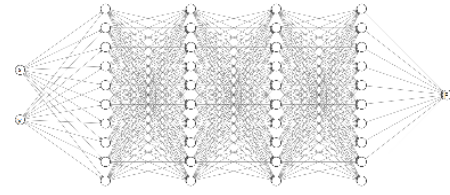
For a scalar function $E(x, y)$,

$$\nabla \times E = \nabla \times (0, 0, E) = \left(\frac{\partial E}{\partial y}, -\frac{\partial E}{\partial x}, 0 \right)$$

Remark 1: The frequency domain Maxwell's equation can be written as

$$\nabla \times (\nabla \times \boldsymbol{E}) - k^2 \boldsymbol{E} = \boldsymbol{0}$$

where $\boldsymbol{E} = (E_x, E_y, E_z)$ is the electronic field. In this paper, we consider TM_z mode, hence $E_x = E_y = 0$. In this case,

FIGURE 1. Diagram of NN with only 10 neurons in the hidden layers. In our experiment, we take 100 neurons.

we can reduce this equation to (1). In this section, we only consider (1) instead of its double curl form.

In the following subsection, we set $\Omega = [0, 1]^2$ and $E_w(x, y) = \sin(kx)$.

C. PINN FOR FREQUENCY DOMAIN MAXWELL'S EQUATION

As suggested in [2], [9], we use a fully connected neural network (NN) with 6 layers, where the input layer contains two neurons denote x and y, output layer contains one neuron denotes the prediction of E and four hidden layers with 100 neurons each. Actually, in [2], [9] the authors tried different neural network structures with different number of layers and neurons. It turns out that when the number of layers and neurons is increasing, the accuracy is almost increasing.

In detail, let l_n denotes the column vector at the nth layer. Then, we have $l_1 = (x, y)^\top, l_6 = E$ and l_i are 100×1 column vectors for $i = 2, 3, 4, 5$. The mathematical relationship between each layer is given by

$$l_{n+1} = \sigma(W_n l_n + b_n) \quad n = 1, 2, 3, 4$$

and

$$l_6 = W_5 l_5 + b_5$$

Here W_n and b_n denote the parameters going to be trained at nth layer. Let l_n be a $m_1 \times 1$ vector, that is, there are m_1 neurons at nth layer, and l_{n+1} be a $m_2 \times 1$ vector (m_2 neurons at $(n+1)$th layer), then we have W_n is a $m_2 \times m_1$ matrix and b_n be a $m_2 \times 1$ vector, which is called bias. $\sigma(\cdot)$ is a vector valued function, which is called the activation function. Let $\sigma(\cdot) : \mathbb{R} \mapsto \mathbb{R}$ be a real value scalar function, then $\sigma(\boldsymbol{x}) = (\sigma(x_1), \sigma(x_2), \cdots, \sigma(x_n))^\top$ where $\boldsymbol{x} = (x_1, x_2, \cdots, x_n)^\top$. For the sake of simplicity, we will just call $\sigma(\cdot)$ as the activation function because it determines the $\boldsymbol{\sigma}(\cdot)$ uniquely. The b_n has been initialized by zero vector and W_n has been initialized by Xavier. Namely, if W_n is an $m_2 \times m_1$ dimensional matrix, we initialized it by a truncated normal distribution with mean 0 and variance $\frac{2}{m_1 + m_2}$. See [10] for more detail. To demonstrate the NN more concretely, we show a diagram of our NN in Figure 1. Notice that there are only 10 neurons in the hidden layers at Figure 1. In our experiments, we will take 100 neurons at each layer as suggested in [9]. We will also discuss the structure of NN in the following numerical experiments.

Besides, we shift and scale the input linearly for each layer to $[-1, 1]$ in order to protect the NN from overfitting and

gradient vanish and blow up. This is the choice shown in [2], [9] and the relationship between width as well as number of neurons for each layer and the accuracy of the result has been studied thereby. So here we follow their choice.

The mean square error (*MSE*), or loss function, is given by

$$MSE = MSE_E + MSE_f$$

$$= \frac{1}{N_E} \sum_{i=1}^{N_E} |E(x_E^i, y_E^i) - E^i|^2 + \frac{1}{N_f} \sum_{i=1}^{N_f} |F(x_f^i, y_f^i)|^2$$

Here $\{x_E^i, y_E^i, E^i\}$ denotes the boundary training data of $E(x, y)$ and $\{x_f^i, y_f^i\}$ denotes the collocation points for

$$F(x, y) = \Delta E + k^2 E$$

in Ω. The $E(x, y)$ in the *MSE* means the NN prediction at given point (x, y). With the automatic differentiation (AD) technique [11], the partial derivative terms in the $F(x, y)$ can be computed easily by just calling the function `tf.gradient` in Tensorflow. Notice that the output E (or, l_6) is a function of the input x and y, (or, l_1) and this function is parametrized by a set of unknowns W_n and b_n, $n = 1, 2 \cdots 5$. And the partial derivative of E is nothing but just apply the chain rule on the NN with respect to the input x and y somehow, so it is still a function of x and y and parameterized by $\{W_n, b_n\}_{n=1}^5$. Therefore, given the training set mentioned above, *MSE* is a function of $\{W_n, b_n\}_{n=1}^5$. We then get the optimization problem from NN: finding $\{W_n, b_n\}_{n=1}^5$ to minimize the *MSE*.

In [2], [9], the activation function $\sigma(s) = \sin(s)$ shows an excellent behavior that solves all of the PDEs' problems thereby. The authors of those two papers mentioned this activation function works stably. For the frequency domain Maxwell's equation, this method works when wave number is not relative high, i.e., $k = 5$. However, when we set $k = 11$, the result shows as Figure 2. We get this result by setting $N_E = 200$, $N_f = 20000$ and train the NN in 5000 iterations by Adam algorithm. After that, we use the L-BFGS packed in SciPy package continues the optimization until the absolute value of difference between loss functions in the consecutive two steps less than 10^{-16}. The points on the boundary are chosen randomly and the points in the interior are chosen by Latin hypercube sampling (LHS). All the computation has been done with Tensorflow 1.13 and run on Amazon web services (AWS) p3.2xlarge. At the final step, $MSE \approx 0.5$. Once again, how the number of training sets and training steps impact the accuracy of the result is still not completely clear. What we can say is that more training sets lead to a relative high accuracy and less overfitting, or more stable. More experimental detail can be found in [2], [9].

After investigating the detail of the NN, we found that the issue is that when k is relatively large, the NN cannot get close to the true W_n, because their initial values are around 0. Notice that the input is between $[-1, 1]$, and the activation function is not in this domain, this probably causes the NN
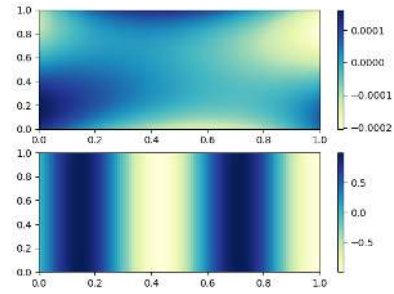

FIGURE 2. Solution $E(x, y)$ by setting $\sigma(s) = \sin(s)$, $k = 11$. Top: Prediction of NN. Underneath: Exact solution.
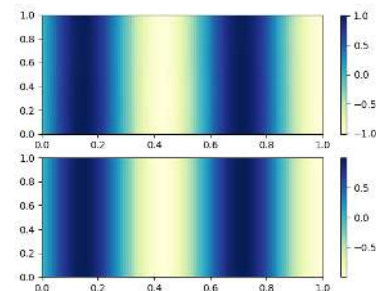

FIGURE 3. Solution $E(x, y)$ by setting $\sigma(s) = \sin(\pi s)$, $k = 11$. Top: Prediction of NN. Underneath: Exact solution.
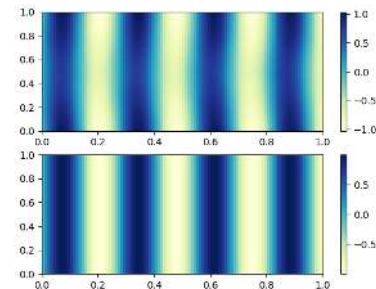

FIGURE 4. Solution $E(x, y)$ by setting $\sigma(s) = \sin(\pi s)$, $k = 23$. Top: Prediction of NN. Underneath: Exact solution.

fails to work. If this conjecture is true, we can fix it by using $\sigma(s) = \sin(\pi s)$ as it is in $s \in [-1, 1]$. We verify this activation function by the same test setting and the result is shown in Figure 3. At the final step, $MSE \approx 10^{-5}$.

We also try a higher wave number $k = 23$ and keep all the other setting same. It turns out that at the final step, the $MSE \approx 0.1$ and the solution is shown in Figure 4. The solution is not as good as the last test but we suggest that this can be improved by using more training samples and training steps.

In the next section, we consider the metamaterial design problems with wave number no more than 11. Hence, this activation function is convinced in this case.

Remark 2: As we know, the mathematical foundation of NN is rare at this time. Hence, the reason that the activation function $\sigma(s) = \sin(s)$ used in [9] fail to work in the aforementioned test is just a conjecture without any proof and then verify by computation. Therefore, in this paper, we just accept
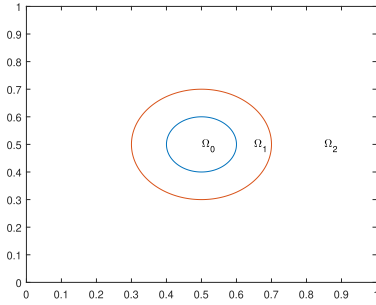
FIGURE 5. Diagram of computational domain.

it 'sloppily' as it really pass the computational test. The proof remains a future work.

Other works we want to mention include [5], [12]–[29].

III. METAMATERIAL DESIGN PROBLEMS

In this section, we consider a PINN identification problem corresponding to the frequency domain Maxwell's equation. Consider the equation

$$\nabla \times (\boldsymbol{\mu}_r^{-1} \nabla \times E) - k^2 \epsilon_r E = F_1 \quad \text{in } \Omega \setminus \Omega_0$$
$$E = E_{in} \quad \text{on } \partial \Omega_0$$
$$E = E_w \quad \text{on } \partial \Omega_2 \setminus \Omega_1 \quad (2)$$

in the domain given by Figure 5, where $E_w(x, y)$ is the given source wave and

$$F_1 = \begin{cases} 0 & \text{in } \Omega_1 \\ \nabla \times \nabla \times E_w - k_0^2 E_w & \text{in } \Omega_2 \end{cases}$$

Here $\boldsymbol{\mu}_r$ and ϵ_r are the relative permeability and permittivity going to design, respectively. $E_{in}(x, y)$ is a given function. If $E_{in}(x, y) = 0$, we get the cloaking problem and if set $E_{in}(x, y)$ as a polar rotation of $E_w(x, y)$, we get the rotator problem.

Note that if we set $\epsilon_r = 1$ and

$$\boldsymbol{\mu}_r = \begin{pmatrix} 1 & 0 \\ 0 & 1 \end{pmatrix}$$

we arrive at (1). Our goal in this section is to find a suitable $\boldsymbol{\mu}_r(x, y)$ and $\epsilon_r(x, y)$ that satisfy (2). By [30], we can make the following assumption on $\boldsymbol{\mu}_r$:

$$\boldsymbol{\mu}_r = \begin{pmatrix} \mu_1(x, y) & \mu_2(x, y) \\ \mu_2(x, y) & \mu_3(x, y) \end{pmatrix}$$

So, our goal now is to find μ_1, μ_2, μ_3 and ϵ_r that satisfy (2). In this section, we set $\Omega_0 \cup \Omega_1 \cup \Omega_2 = [-2, 2]^2$.

A. CLOAKING PROBLEM

In this subsection, we consider cloaking problem $E_{in}(x, y) = 0$. We first point out that the PEC condition is usually $\boldsymbol{n} \times E = \boldsymbol{0}$ on the boundary. But we are working at TM_z mode, say, $E = (0, 0, E(x, y))$, that is equivalent to $E(x, y) = 0$ in our problem. We set our geometry as follow: $\Omega_0 = \{\boldsymbol{x} : \|\boldsymbol{x}\|_{\mathbb{R}^2} \leq 0.3\}$, $\Omega_1 = \{\boldsymbol{x} : 0.3 < \|\boldsymbol{x}\|_{\mathbb{R}^2} \leq 0.6\}$ and
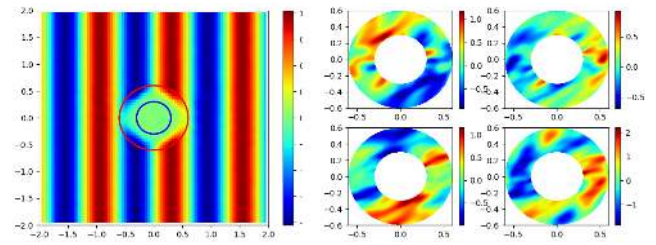

FIGURE 6. Cylindrical cloak, $k = 5$. (a) Left: $E(x, y)$. (b) Right: From up left to down right: μ_1, μ_2, μ_3 and ϵ_r.

$\Omega_2 = \{\boldsymbol{x} \in [-2, 2]^2 : \|\boldsymbol{x}\|_{\mathbb{R}^2} > 0.6\}$, where $\| \cdot \|_{\mathbb{R}^2}$ denotes the Euclidean norm in $\mathbb{R}^2$ and $\boldsymbol{x} = (x, y)$.

To find out a suitable function $\boldsymbol{\mu}_r(x, y)$ and $\epsilon_r(x, y)$ that satisfy (2), we setup another NN for them. This NN has almost same structure to the one solving (1). The only difference is that the output layer contains four neurons for μ_1, μ_2, μ_3 and ϵ_r, respectively.

The cloaking problem is that given a wave source, we would like to keep it outside the metamaterial which includes a conductor inside. Based on this, our loss function reads

$$MSE = MSE_f + MSE_c$$
$$= \frac{1}{N_f} \sum_{i=1}^{N_f} |g(x_f^i, y_f^i)|^2 + \frac{1}{N_c} \sum_{i=1}^{N_c} |E(x_c^i, y_c^i) - E_{in}^i|^2$$

They satisfy the frequency domain Maxwell's equation in the vacuum with the given source as the boundary condition. The $E(x, y)$ in the MSE means the NN prediction of E at point (x, y). $\{x_f^i, y_f^i\}$ denotes the collocation points for

$$g(x, y) = \nabla \times (\boldsymbol{\mu}_r^{-1}(x, y) \nabla \times E(x, y)) - k^2 \epsilon_r E(x, y)$$

in $\Omega_1 \cup \Omega_2$. And $\{x_c^i, y_c^i, E_{in}^i\}$ denotes boundary data at $\partial \Omega_0$, namely, PEC boundary condition in this test.

We consider $k = 5$ and set $N_f = 20000$ and $N_c = 1000$ and train the NN by 10000 steps. The result is shown in Figure 6. We predict $E(x, y)$ by using 200000 points in Ω as shown in Figure 6 (a). The metamaterial design is shown in Figure 6 (b). At the final step, the $MSE \approx 10^{-5}$. We point out some flaws of this method. First, as shown in Figure 6 (b), the patterns of metamaterial are almost random, this entail our result is only a theoretical one instead of practical. Second, we find that on some regions $\mu_i = 0$ for $i = 1, 2, 3$. This makes the $\boldsymbol{\mu}_r^{-1}$ has a non desirable behavior, and sometimes $\boldsymbol{\mu}_r$ even not invertible. But this situation is also happened in the exact solution of cylindrical cloaking. As suggested in [30], the polar components of metamaterial for perfect cloaking reads

$$\epsilon_r = \mu_r = \frac{r - R_1}{r}, \quad \epsilon_\phi = \mu_\phi = \frac{r}{r - R_1}$$
$$\epsilon_z = \mu_z = \left(\frac{R_2}{R_2 - R_1} \right)^2 \frac{r - R_1}{r}$$

where R_1 and R_2 are the inner and outer radius of the annular. Hence, we observe that when $r \to R_1$, $\epsilon_\phi \to \infty$.

TABLE 1. Value of loss function for cross-validation with different PINNs' structures for cloaking problem.

Neurons / Layers	10	20	30	40	50	60	70	80	90	100
2	$2.30E-04$	$1.65E-04$	$2.70E-04$	$2.97E-04$	$1.94E-04$	$1.26E-04$	$1.13E-04$	$4.65E-05$	$2.69E-05$	$2.43E-05$
4	$8.76E-06$	$2.93E-06$	$2.23E-06$	$1.99E-06$	$1.49E-06$	$1.00E-06$	$6.29E-07$	$5.23E-07$	$2.55E-07$	$2.26E-07$
6	$2.82E-05$	$4.04E-06$	$2.79E-06$	$1.80E-06$	$1.63E-06$	$1.30E-06$	$8.17E-07$	$2.96E-07$	$2.22E-07$	$1.57E-07$
8	$7.84E-06$	$2.85E-06$	$2.38E-06$	$1.75E-06$	$9.27E-07$	$3.99E-07$	$2.51E-07$	$1.54E-07$	$8.03E-08$	$2.62E-08$
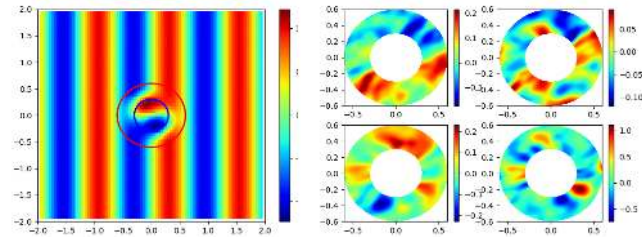
FIGURE 7. Cylindrical rotator, $k = 5$. (a) Left: $E(x, y)$. (b) Right: From up left to down right: μ_1, μ_2, μ_3 and ϵ_r.

FIGURE 8. Cylindrical rotator, $k = 11$. (a) Left: $E(x, y)$. (b) Right: From up left to down right: μ_1, μ_2, μ_3 and ϵ_r.

Nevertheless, these two defects can be conquered by using piecewise constant design problem. See section IV of this paper below. Finally, suppose we get a valid solution μ_r and ϵ_r, then $-\mu_r$ and $-\epsilon_r$ are also solutions due to equation (2). This may cause the result unstable mathematically.

Finally, we study the relationship between the accuracy and structure of PINNs. As the work shown in [9], we change the number of layers and neurons for each layer for both E and permittivity and permeability at the same time. And then keep all the other settings as the same. After training the PINNs, we use another set of randomly generated data with same sample size to do the cross-validation. Since there is no exact solution of our problem, we show the value of loss function in table 1. As shown in the table, although there are few exceptions, when the number of layers and neurons are increasing, the accuracy is almost increasing. This fit the results in [2], [9]. To balance the workload and accuracy, we will adopt the setting in [9]. That is, 6 layers with 100 neurons with each layers will be used in the numerical experiments below. In a practical problem, one can choose different PINNs structure and sample size to balance the workload, accuracy and capacity of PINNs in the specific case.

B. ROTATOR

In this subsection, we consider another metamaterial design problem. Given a source wave on Ω_2, our target now is rotating the wave by a certain degree. In this subsection, we set this degree as $\frac{\pi}{2}$. We keep all other setting as the same to the last experiment except for $E_{in}(x, y) = \sin(ky)$. When $k = 5$, the result is shown in Figure 7.

As mentioned previously, the activation function $\sigma(s) = \sin(\pi s)$ may conquer the relative high wave number difficulty in the frequency domain Maxwell's equation. Here, we test it by our metamaterial design for the rotator problem. We change $k = 11$, and the results are shown in Figure 8.
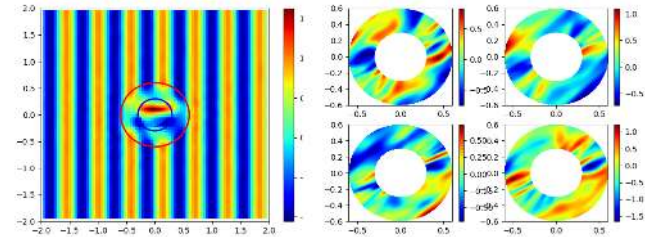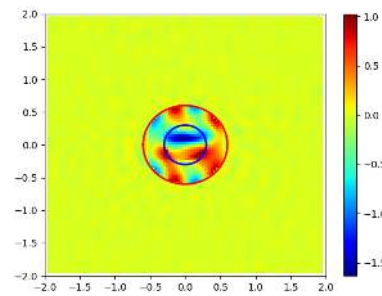
FIGURE 9. Scatter field of $E(x, y)$.

We also plot the scatter field to show the error of this solution in Figure 9. All of the $MSE \approx 10^{-5}$ at these two tests in this section.

Although we adopt the 6 layers and 100 neurons structure, loss function values with different network structure has been shown in table 2. Once again, the larger network almost gives more accuracy.

IV. DISCRETE DESIGN FOR CLOAKING

As mentioned in the previous section, the continuous design for cloaking metamaterial has many defects. As suggested in [30], [31], when we approximate the exact solution μ_r and ϵ_r for cloaking by piecewise constant functions in polar coordinate, we may get almost cloaking metamaterial. This enlighten us to design the metamaterial by using piecewise functions on a certain partition. If this can be done, we may manufacture this metamaterial and then our result is more practical. This experiment follow the work in [30]–[34], which is the benchmark problem in electromagnetic cloaking area. Namely, we have used almost same geometry to those work but different sizes.

Let Ω_0 be a disc centered at origin with radius $0.3m$, and Ω_1 be an annulus with inner radius $0.3m$ and outer radius $0.6m$. And we set $\Omega_0 \cup \Omega_1 \cup \Omega_2 = [-2, 2]m \times [-2, 2]m$. To design a piecewise constant metamaterial, we partition the Ω_1 into 8

TABLE 2. Value of loss function for cross-validation with different PINNs' structures for rotator problem.

Layers \ Neurons	10	20	30	40	50	60	70	80	90	100
2	$3.43E-04$	$2.33E-04$	$3.90E-04$	$4.41E-04$	$3.02E-04$	$1.93E-04$	$1.77E-04$	$7.03E-05$	$4.09E-05$	$3.71E-05$
4	$1.31E-05$	$4.20E-06$	$3.43E-06$	$3.01E-06$	$2.26E-06$	$1.59E-06$	$9.49E-07$	$7.93E-07$	$3.96E-07$	$3.65E-07$
6	$4.23E-05$	$6.12E-06$	$3.84E-06$	$2.69E-06$	$2.54E-06$	$1.99E-06$	$1.19E-06$	$4.63E-07$	$3.27E-07$	$2.36E-07$
8	$1.08E-05$	$4.51E-06$	$3.40E-06$	$2.58E-06$	$1.49E-06$	$5.80E-07$	$4.01E-07$	$2.34E-07$	$1.14E-07$	$3.74E-08$

annulus with same thickness, say, $(0.6 - 0.3)/8 = 0.0375m$. Since the components of μ_r and ϵ_r are piecewise constants in polar coordinate as in [30], [31], we now transform our governor equation to polar coordinate:

$$\frac{1}{r}\frac{\partial}{\partial r}\left(\frac{r}{\mu_\phi}\frac{\partial E}{\partial r}\right) + \frac{1}{r^2}\frac{\partial}{\partial \phi}\left(\frac{1}{\mu_r}\frac{\partial E}{\partial \phi}\right) + k^2\epsilon_z E = F_2 \text{ in } \Omega$$
$$E = E_{in} \text{ on } \partial\Omega_0$$
$$E = E_w \text{ on } \partial\Omega_2 \setminus \partial\Omega_1 \qquad (3)$$

where $E(r, \phi)$ is the electronic field in polar coordinate and μ_ϕ, μ_r and ϵ_z are the polar components of permittivity and permeability, respectively. The right hand side term F_2 has been defined as

$$F_2 = \begin{cases} 0 & \text{in } \Omega_1 \\ \frac{1}{r}\frac{\partial}{\partial r}\left(\frac{r}{\mu_\phi}\frac{\partial E_w}{\partial r}\right) + \frac{1}{r^2}\frac{\partial}{\partial \phi}\left(\frac{1}{\mu_r}\frac{\partial E_w}{\partial \phi}\right) + k^2\epsilon_z E_w & \\ & \text{in } \Omega_2 \end{cases}$$

We choose a P band sinusoidal source wave with frequency 0.23873GHz, and assume the Ω_0 is a perfect electronic conductor. We use the same loss function and NN structure but just change the input from x and y to r and ϕ. The bottom line in this problem is how we recover a sort of piecewise constant functions by NN? Indeed, we can still predict these functions by NN and put penalty terms in the loss function to enforce the desired functions has no variance on each subdomain. But this obviously add more workload because we only need one variable on each subdomain but get many from NN if we do so. Enlightened by [9], we can mimic the idea of PINN identification. We set only one variable on each subdomain which is exactly what we need. To elaborate this idea, we begin with one dimensional piecewise constant function approximation.

Consider the piecewise constant function $f(x)$ defined as

$$f(x) = \begin{cases} y_0 & x \in [x_0, x_1] \\ y_1 & x \in (x_1, x_2] \\ \dots & \\ y_{n-1} & x \in (x_{n-1}, x_n] \end{cases}$$

Let $\chi_{[x_i,x_{i+1}]}(x) = \chi_{(x_i,x_{i+1}]}(x)$ denotes the indicator function on $[x_i, x_{i+1}]$ or $(x_i, x_{i+1}]$ and $\widetilde{\chi}_i(x)$ the modified sigmoid function:

$$\widetilde{\chi}_i(x; a) = \frac{1}{1 + e^{a(x-x_i)}}$$

where $a > 0$ is the scaling parameter. It follows that

$$\chi_{[x_i,x_{i+1}]}(x) \approx \widetilde{\chi}_i(x; a) - \widetilde{\chi}_{i+1}(x; a)$$

TABLE 3. Design of piecewise constant metamaterial (from left to right is inner to outer layer).

μ_ϕ	μ_r	ϵ_z
-1.5097	4.0955	1.5112
-3.4218	76.9249	0.4732
80.5069	52.9568	0.0042
15.0861	7.0880	0.1083
1.6152	0.7103	1.1361
1.4486	0.7606	1.1083
1.6759	1.1431	0.7815
1.1514	0.9953	0.9533

TABLE 4. Piecewise constant metamaterial given by perfect cloaking formula (from left to right is inner to outer layer).

μ_ϕ	μ_r	ϵ_z
17.0000	0.0588	0.2353
6.3333	0.1579	0.6316
4.2000	0.2381	0.9524
3.2857	0.3043	1.2174
2.7778	0.3600	1.4400
2.4545	0.4074	1.6296
2.2308	0.4483	1.7931
2.0667	0.4839	1.9355

when a large enough. Hence, we may approximate the $f(x)$ by using $\widetilde{\chi}_i(x; a)$:

$$f(x) = \sum_{i=1}^{n-1} y_i \chi_{[x_i,x_{i+1}]}(x)$$
$$\approx \sum_{i=1}^{n-1} y_i(\widetilde{\chi}_i(x; a) - \widetilde{\chi}_{i+1}(x; a))$$
$$= \sum_{i=1}^{n-1}(y_i - y_{i-1})\widetilde{\chi}_i(x; a) + y_0\widetilde{\chi}_0(x; a) - y_{n-1}\widetilde{\chi}_n(x; a)$$
$$(4)$$

Back to our metamaterial design problem. We set our desired functions μ_ϕ, μ_r and ϵ_z by using (4), where y_is in (4) are variables in Tensorflow. Take μ_ϕ as an example, we set

$$\mu_\phi(r) = \sum_{i=1}^{7}(\mu_{\phi,i} - \mu_{\phi,i-1})\widetilde{\chi}_i(r; a)$$
$$+ \mu_{\phi,0}\widetilde{\chi}_0(r; a) - \mu_{\phi,7}\widetilde{\chi}_7(r; a)$$

where $r = \sqrt{x^2 + y^2}$. In our experiment, we choose $a = 100 \times \frac{\Delta r}{6}$, where Δr is the thickness of the metamaterial. We set $N_f = 30000$ and $N_c = 1000$ and train the NN by 10000 steps. The result is shown in Figure 10. Figure 10 (a) shows the electronic field $E(x, y)$ with piecewise constant cloaking metamaterial. As shown in the figure, the source

TABLE 5. Value of loss function for cross-validation with different PINNs' structures for discrete design cloaking problem.

Neurons / Layers	10	20	30	40	50	60	70	80	90	100
2	$1.49E-02$	$1.10E-02$	$1.67E-02$	$1.97E-02$	$1.27E-02$	$8.88E-03$	$8.18E-03$	$3.16E-03$	$1.71E-03$	$1.73E-03$
4	$6.10E-04$	$1.80E-04$	$1.48E-04$	$1.22E-04$	$9.68E-05$	$6.69E-05$	$4.16E-05$	$3.47E-05$	$1.78E-05$	$1.57E-05$
6	$1.83E-03$	$2.51E-04$	$1.83E-04$	$1.24E-04$	$1.16E-04$	$8.49E-05$	$5.28E-05$	$2.06E-05$	$1.46E-05$	$1.09E-05$
8	$4.83E-04$	$1.86E-04$	$1.58E-04$	$1.09E-04$	$6.69E-05$	$2.61E-05$	$1.73E-05$	$1.10E-05$	$5.05E-06$	$1.66E-06$
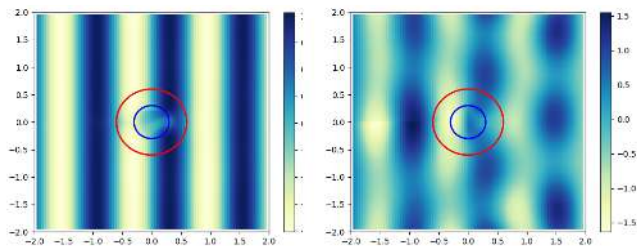
FIGURE 10. Piecewise constant cloaking, $k = 5$. (a) Left: $E(x, y)$ with metamaterial. (b) Right: $E(x, y)$ without metamaterial.
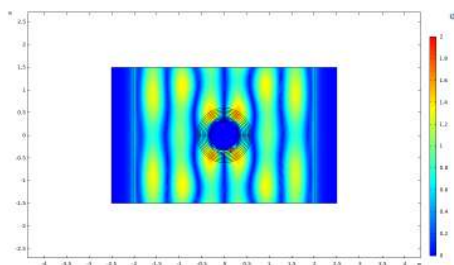
FIGURE 11. $E(x, y)$ by Comsol. Permittivity and permeability are given by the piecewise constant solution of NN.

wave has been kept in Ω_2. The metamaterial shell Ω_1 ensure that the wave inside Ω_0 is identically 0. Consequently, we can put an object with any shape and material in Ω_0 without disturbing the incident wave. That is, the object can be cloaked in the electromagnetic field. As a comparison, we also put a solution $E(x, y)$ without any metamaterial in Figure 10 (b). Namely, in 10 (b), Ω_1 is a conductor with PEC on $\partial\Omega_1$ and $\Omega_2 \cup \Omega_3$ is vacuum. The result of metamaterial is shown in Table 3. To assure this result is true, we resolve this model in Comsol 5.4 by using the metamaterial in Table 3, and the result is shown in Figure 11. As shown in the figure, the wave almost keep the same although the little deformation.

We display the result given by the perfect cloaking formula in Table 4. Comparing Table 1 and Table 2, we know that the NN gives us a different solution to the perfect cloaking formula. We also point out that the sign of the metamaterial still cannot be decided. That is, if μ_ϕ, μ_r and ϵ_z is a set of solution, $-\mu_\phi$, $-\mu_r$ and $-\epsilon_z$ is also a set of solution.

Similar to the previous two metamaterial design problem, we show the loss function values with varied network structures as shown in 5. Again, we find that larger network gives more accuracy.

V. CONCLUSION

This paper studies the PINN inference problems for the frequency domain Maxwell's equation and the identification problems for the electromagnetic metamaterial design.

These problems are widely used in physical and engineering areas. The universal framework of PINN for inference and identification problems are discussed in [9]. We adopt this idea and improve the activation function to conquer the high wave number problems. Additionally, what we recovered are continuous functions and piecewise constant functions. This is a new contribution for the application of PINN in practical problems. Finally, we point out that by using NN methods, we figure out new solutions which are differ from the ones in [30]. As those solution pass the test of Comsol, they are reliable.

We conclude this paper by pointing out some potential future works. First, we may use our method to solve metamaterial design problems with more complex domains, as the examples in [35]. Second, the perfect cloaking design supposes to absorb the wave from any direction with any frequency theoretically. However, as we mentioned, the current method cannot achieve this. Some physical restrictions should be added in the loss functions. For example, the Brewster's angle may protect the result from reflection. Finally, we may apply this approach to other electromagnetic problems in engineering and physics. For example, given that there is a conductor somewhere in an area, we may use the sensor's data to recover the location of the conductor as well as its geometry probably. This is so-called scattering problems.

REFERENCES

[1] J. B. Pendry, "Negative refraction makes a perfect lens," *Phys. Rev. Lett.*, vol. 85, no. 18, pp. 3966–3969, Jul. 2002.

[2] M. Raissi and G. E. Karniadakis, "Hidden physics models: Machine learning of nonlinear partial differential equations," *J. Comput. Phys.*, vol. 357, pp. 125–141, Mar. 2018.

[3] R. Walser, "Electromagnetic metamaterials in complex mediums II: Beyond linear isotropic dielectrics," *Int. Soc. Opt. Photon.*, vol. 4467, no. 18, pp. 1–16, 2001.

[4] J. B. Pendry, "Controlling electromagnetic fields," *Science*, vol. 312, no. 5781, pp. 1780–1782, Jun. 2006.

[5] J. D. Murray, *Mathematical Biology II: Spatial Models and Biomedical Applications*. New York, NY, USA: Springer, 2003

[6] M. Rastegari, V. Ordonez, J. Redmon, and A. Farhadi, "XNOR-Net: ImageNet classification using binary convolutional neural networks," in *Proc. Eur. Conf. Comput. Vis.*, vol. 314, no. 5801. Cham, Switzerland: Springer, Oct. 2016, pp. 525–542.

[7] E. Gawehn, J. A. Hiss, and G. Schneider, "Deep learning in drug discovery," *Mol. Inf.*, vol. 35, no. 1, pp. 3–14, Jan. 2016.

[8] B. Alipanahi, A. Delong, M. Weirauch, and B. Frey, "Predicting the sequence specificities of DNA-and rna-binding proteins by deep learning," *Nature Biotechnol.*, vol. 33, no. 8, p. 831, 2015.

[9] M. Raissi, P. Perdikaris, and G. Karniadakis, "Physics-informed neural networks: A deep learning framework for solving forward and inverse problems involving nonlinear partial differential equations," *J. Comput. Phys.*, vol. 378, pp. 686–707, Feb. 2019.

[10] X. Glorot and Y. Bengio, "Understanding the difficulty of training deep feedforward neural networks," in *Proc. 13th Int. Conf. Artif. Intell. Statist.*, Mar. 2010, vol. 314, no. 5801, pp. 249–256.

[11] A. G. Baydin, B. A. Pearlmutter, A. A. Radul, and J. M. Siskind, "Automatic differentiation in machine learning: A survey," *J. Mach. Learn. Res.*, vol. 18, pp. 1–43, Apr. 2018.

[12] M. Bhaduri and J. Zhan, "Using empirical recurrence rates ratio for time series data similarity," *IEEE Access*, vol. 6, pp. 30855–30864, 2018.

[13] M. Bertalmio, L. T. Cheng, S. Osher, and S. Guillermo, "Variational problems and partial differential equations on implicit surfaces: The framework and examples in image processing and pattern formation," *J. Comput. Phys.*, Vol. 174, no. 2, pp. 759–780, Dec. 2001.

[14] P. Ezatpoor, J. Zhan, J. M.-T. Wu, and C. Chiu, "Finding top-*k* dominance on incomplete big data using mapreduce framework," *IEEE Access*, vol. 6, pp. 7872–7887, 2018.

[15] P. Chopade and J. Zhan, "A framework for community detection in large networks using game–theoretic modeling," *IEEE Trans. Big Data*, vol. 3, no. 3, pp. 276–288, Sep. 2017.

[16] M. Bhaduri, J. Zhan, and C. Chiu, "A novel weak estimator for dynamic systems," *IEEE Access*, vol. 5, pp. 27354–27365, 2017.

[17] M. Bhaduri, J. Zhan, C. Chiu, and F. Zhan, "A novel online and non–parametric approach for drift detection in big data," *IEEE Access*, vol. 5, pp. 15883–15892, 2017.

[18] C. Chiu, J. Zhan, and F. Zhan, "Uncovering suspicious activity from partially paired and incomplete multimodal data," *IEEE Access*, vol. 5, pp. 13689–13698, 2017.

[19] J. M.-T. Wu, J. Zhan, and J. C.-W. Lin, "Ant colony system sanitization approach to hiding sensitive itemsets," *IEEE Access*, vol. 5, pp. 10024–10039, 2017.

[20] J. Zhan and B. Dahal, "Using deep learning for short text understanding," *J. Big Data*, vol. 4, no. 1, Dec. 2017.

[21] J. Zhan, S. Gurung, and S. P. K. Parsa, "Identification of top-K nodes in large networks using Katz centrality," *J. Big Data*, vol. 4, no. 1, p. 16, Dec. 2017.

[22] J. Zhan, T. Rafalski, G. Stashkevich, and E. Verenich, "Vaccination allocation in large dynamic networks," *J. Big Data*, vol. 4, no. 1, p. 2, Dec. 2017.

[23] H. Selim and J. Zhan, "Towards shortest path identification on large networks," *J. Big Data*, vol. 3, no. 1, p. 10, Dec. 2016.

[24] F. Zhan, A. Martinez, N. Rai, R. Mcconnell, M. Swan, M. Bhaduri, J. Zhan, L. Gewali, and P. Oh, "Beyond cumulative sum charting in non–stationarity detection and estimation," *IEEE Access*, vol. 7, pp. 140860–140874, 2019.

[25] A. Hart, B. Smith, S. Smith, E. Sales, J. Hernandez-Camargo, Y. M. Garcia, F. Zhan, L. Griswold, B. Dunkelberger, M. R. Schwob, S. Chaudhry, J. Zhan, L. Gewali, and P. Oh, "Resolving intravoxel white matter structures in the human brain using regularized regression and clustering," *J. Big Data*, vol. 6, no. 1, p. 61, Dec. 2019.

[26] F. Zhan, "Hand gesture recognition with convolution neural networks," in *Proc. IEEE 20th Int. Conf. Inf. Reuse Integr. Data Sci. (IRI)*, Jul./Aug. 2019.

[27] F. Zhan, "How to optimize social network influence," in *Proc. IEEE 2nd Int. Conf. Artif. Intell. Knowl. Eng. (AIKE)*, Cagliari, Italy, Jun. 2019.

[28] E. Aguilar, J. Dancel, D. Mamaud, D. Pirosch, F. Tavacoli, F. Zhan, R. Pearce, M. Novack, H. Keehu, B. Lowe, J. Zhan, L. Gewali, and P. Oh, "Highly parallel seedless random number generation from arbitrary thread schedule reconstruction," in *Proc. IEEE Int. Conf. Big Knowl.*, Beijing, China, Nov. 2019.

[29] E. Hunt, R. Janamsetty, C. Kinares, C. Koh, A. Sanchez, F. Zhan, M. Ozdemir, S. Waseem, O. Yolcu, B. Dahal, J. Zhan, L. Gewali, and P. Oh, "Machine learning models for paraphrase identification and its applications on plagiarism detection," in *Proc. IEEE Int. Conf. Big Knowl.*, Beijing, China, Nov. 2019.

[30] S. A. Cummer, B.-I. Popa, D. Schurig, D. R. Smith, and J. Pendry, "Full-wave simulations of electromagnetic cloaking structures," *Phys. Rev. E, Stat. Phys. Plasmas Fluids Relat. Interdiscip. Top.*, vol. 74, no. 3, Sep. 2006, Art. no. 036621.

[31] K. Klasing, D. Althoff, D. Wollherr, and M. Buss, "Comparison of surface normal estimation methods for range sensing applications," in *Proc. IEEE Int. Conf. Robot. Automat.*, Kobe, Japan, May 2009, pp. 3206–3211.

[32] X. Zhou and G. Hu, "Design for electromagnetic wave transparency with metamaterials," *Phys. Rev. E, Stat. Phys. Plasmas Fluids Relat. Interdiscip. Top.*, vol. 74, no. 2, Aug. 2006, Art. no. 026607.

[33] M. Rahm, D. Schurig, D. A. Roberts, S. A. Cummer, D. R. Smith, and J. B. Pendry, "Design of electromagnetic cloaks and concentrators using form-invariant coordinate transformations of Maxwell's equations," *Photon. Nanostruct. Fundam. Appl.*, vol. 6, no. 1, pp. 87–95, Apr. 2008.

[34] Y. Liu, B. Gralak, and S. Guenneau, "Finite element analysis of electromagnetic waves in two-dimensional transformed bianisotropic media," *Opt. Express*, vol. 24, no. 23, p. 26479, Nov. 2016.

[35] J. Hu, X. Zhou, and G. Hu, "Calculation of material properties for arbitrary shape transformation media," in *Proc. Int. Workshop Metamater.*, Nov. 2008, pp. 118–121.

ZHIWEI FANG is currently pursuing the Ph.D. degree in mathematics with the Department of Mathematical Sciences, University of Nevada at Las Vegas, Las Vegas, NV, USA. His research interests include machine learning, numerical methods for partial differential equations, computational electromagnetic fields, and uncertainty quantification.

JUSTIN ZHAN is currently an ARA Scholar and also a Professor of data science with the Department of Computer Science and Computer Engineering, University of Arkansas. He is also an Adjunct Professor with the Department of Biomedical Informatics, University of Arkansas for Medical Sciences. He has been the Director of the Big Data Hub and a Professor of the Department of Computer Science, College of Engineering, University of Nevada, Las Vegas, NV, USA.

He has published 230 articles in peer-reviewed journals and conferences and has delivered more than 30 keynote speeches and invited talks. He has been involved in more than 50 projects as a principal investigator (PI) or a Co-PI, which were funded by the National Science Foundation, Department of Defense, National Institute of Health, and so on. His research interests include data science, biomedical informatics, artificial intelligence, information assurance, and social computing. He was the Steering Chair of the IEEE International Conference on Social Computing (SocialCom), the IEEE International Conference on Privacy, Security, Risk and Trust (PASSAT), and the IEEE International Conference on BioMedical Computing (BioMedCom). He has served as the Conference General Chair, Program Chair, Publicity Chair, Workshop Chair, and a program committee member for 150 international conferences. He has also served as the editor-in-chief, editor, associate editor, guest editor, editorial advisory board member, and editorial board member for 30 journals. He has been an Editor-in-Chief of the *International Journal of Privacy, Security and Integrity*, and the *International Journal of Social Computing and Cyber-Physical Systems*.

● ● ●